The Molecular Basis for the Relationship between the Secondary Relaxation and Mechanical Properties of a Series of Polyester Copolymer Glasses

Lisa P. Chen and Albert F. Yee*

Macromolecular Science and Engineering, University of Michigan, Ann Arbor, Michigan 48109-2136

Eric J. Moskala

Eastman Chemical Company, Kingsport, Tennessee 37662

Received August 28, 1998; Revised Manuscript Received July 12, 1999

ABSTRACT: A correlation between the yield behavior of copolymers based on poly(ethylene terephthalate) and poly(1,4-cyclohexylenedimethylene terephthalate) (PCT) and their secondary relaxation motions is established. The yield stress decreases as the cyclohexylene content increases for different temperatures and strain rates. The activation volume based on Eyring's model of yielding increases as the copolymers become more PCT-like, while the activation energy does not exhibit any significant change. We speculate that the conformational changes of the cyclohexylene rings reduce the barriers between chain segments sufficiently to facilitate chain slippage. This is supported by the increased dynamic fluctuation found by positron annihilation lifetime spectroscopy. The crazing stress of the copolyesters increases with increasing cyclohexylene content. We propose that the formation of stable microvoids is impeded by local stress relaxation; hence craze formation is retarded. The ductile/brittle transition is viewed as a competition between yielding and crazing with changes in the transition temperature dependent on activation of molecular motions of the cyclohexylene groups.

Introduction

Although it is widely recognized that secondary relaxations of polymers affect macroscopic mechanical properties, the specifics of this relationship are not well defined on a molecular scale. The correlation between the secondary relaxation and mechanical behavior was established on the basis of observations that ductile materials have pronounced low-temperature secondary loss peaks in their dynamic mechanical spectra. The ductile−brittle transition temperature, the temperature or strain rate at which the mode of failure changes from ductile to brittle, was often correlated to secondary relaxation peak temperatures. The broadest review of this correlation was given by Boyer,[1] who compared the temperature dependence of impact strength of several thermoplastics to their respective secondary relaxation peaks and found transitions occurring near loss peak temperatures. Heijboer[2] also compared the impact strengths of polymers with secondary relaxation peaks and noted a major transition in the impact strength. However, he also noted that the temperatures of the secondary loss peaks and the transitions in impact strength could differ considerably. He attributed these differences to the fact that typical impact frequencies lie in the kilohertz range, which can be accessible only with difficulty by dynamic mechanical measurements. That is, to carry out a valid comparison, extrapolation of the dynamic mechanical results into a comparable frequency or time scale is required. This was done by Sacher,[3] who found a good correlation. Others such as Wada and Kasahara[4] related Izod impact strengths for a series of polymers to the areas under their loss peaks, thereby correlating the breadth of the relaxation to impact strength.

Despite the evidence cited above, other researchers have disputed the existence of any correlation.[5−7] Vincent[5] did not observe any ductile−brittle transitions in the temperature range of −20 to 60 °C for the 20 different thermoplastics tested. He did, however, find correlations between the brittle fracture stress and the secondary loss peaks from dynamic mechanical tests; i.e., where the dynamic loss peaks occurred, the brittle fracture stress peaked at these temperatures also. Charpy impact tests conducted on Bisphenol A polycarbonate (BPA-PC) by Glover et al.[6] also showed no signs of a transition between −200 and 50 °C. (The secondary relaxation occurs near −100 °C at 1 Hz.) They observed similar results for slow three-point-bend tests conducted on Charpy-type specimens. Kastelic and Baer[7] investigated the tensile behavior of amorphous poly(ethylene terephthalate) (PET) and BPA-PC over a wide range of temperatures (−273 to 27 °C) and found a mixed correlation. In the case of PET, yielding occurred at temperatures above −73 °C; this is roughly the temperature of the secondary relaxation for PET at 1 Hz. For BPA-PC, however, the specimens were able to yield at temperatures down to −195 °C, clearly far below the secondary relaxation temperature.

The opposing opinions regarding the correlation between the secondary relaxation and impact strength may indeed partly be due to failure to consider the difference in frequency between the varying types of tests, as noted by Heijboer.[2] Because impact test frequencies commonly used lie in the kilohertz range, this can be associated with a shift in the loss peak temperature by as much as several tens of degrees. Unless the issue of frequency equivalence is addressed, comparisons are simply inappropriate. Additionally, external differences lie in the use of different experimental techniques. These range from the type of impact test used to the use of specimen notches and the radii and depth of the notches. Experimental differences such

10.1021/ma981363a CCC: $18.00
Published on Web 08/18/1999

as these can give a wide range of impact strengths with the ductile−brittle transition occurring at seemingly many different temperatures. Those who attempted to find a correlation between secondary relaxations and impact strengths often failed to recognize that the materials were subjected to significantly different stress states due to the difference in specimen and notch geometries. We believe that when these experimental variables are taken into account, a correlation between the ductile−brittle transition temperature and the temperature of the secondary loss peak may well be found to exist.

We, however, are interested in not only establishing this correlation but also, more importantly, understanding how and why the secondary relaxation affects the ductile−brittle transition. Earlier studies have shown that the secondary relaxation of polymers originates from motions of some part of the polymer molecule. We wish to identify the role of these molecular motions in mechanical behavior. Heijboer[2] compared the impact strengths of polymers with secondary relaxation peaks known to be dominated by motions of the side chain to those with loss peaks dominated by main-chain motions. He noted that for the latter a major transition in the impact strength was very likely, while for the former no major effect on the impact strength was observed. Xiao et al. concluded that the cooperative motion of several repeat units giving rise to the secondary loss peak of BPA-PC is key to its ductile behavior and impact strength.[8,9] These studies suggest that molecular scale motions of the secondary relaxation are intimately related to the ductile−brittle transition temperature.

To further explore this relationship, it is worthwhile to better define the ductile−brittle transition. The change from a ductile to a brittle mode of failure can be understood more simply in terms of two competing critical stresses: the brittle stress and the yield stress.[10] A stress system can be described by two components—deviatoric and hydrostatic—both of which contribute to the deformation of the material until failure occurs. How soon a critical stress state is reached determines whether a specimen undergoes brittle failure or ductile failure. On a microscopic level, brittle failure in a thermoplastic is often associated with crazing while ductile failure is associated with shear yielding. The ultimate mode of failure is then the result of a competition between yielding and crazing. If the craze stress is higher than the yield stress, then yielding will be the preferred form of deformation, and the material will fail in a ductile manner. However, if the craze stress is lower than the yield stress, then brittle failure by crazing will ensue. Thus, the focus of this work is actually to understand how molecular motions of the secondary relaxation may affect shear yielding and crazing. A considerable number of studies have attempted to link the secondary relaxation to the yielding process by comparing the activation energies of each. By using the Eyring model for yielding,[11]

$$\frac{\sigma_y}{T} = \frac{\Delta H}{\nu T} + \frac{R}{\nu} \ln \frac{2\dot{\epsilon}}{\dot{\epsilon}_0} \qquad (1)$$

the activation energy and volume, ΔH and ν, respectively, can be determined from plots of the temperature-normalized yield stress (σ_y/T) against the logarithm of the strain rate ($\ln \dot{\epsilon}$) where $R = 1.99$ cal/(mol K) (eq 1). This model was used to fit many plots of parallel, linear

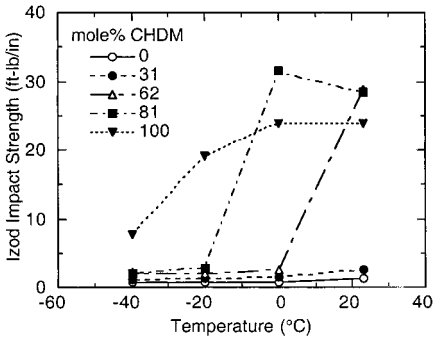

Figure 1. Change in ductile−brittle transition temperatures from Izod impact studies of copolymers with increasing CHDM content

isotherms for several polymers above room temperature.[12−15] Although the model is simplistic and does not offer any molecular descriptions, ΔH and ν give some quantitative understanding of the microscopic process. The secondary relaxation appears to facilitate yielding in some manner, but just how these motions contribute is presently unclear. This is because the description of the flow process of yielding according to the Eyring model is rather ambiguous. The basic molecular process could be either intermolecular (e.g., chain sliding), intramolecular (e.g., a sequence of conformational changes along a chain), or a combination of both.

The relationship between the secondary relaxation and crazing has been little explored. Other than Vincent's observations of a possible correlation between the brittle fracture stress and the secondary loss peak from dynamic mechanical tests,[5] little is known regarding the effect of molecular motions on crazing of bulk polymers. Many studies have been conducted on the crazing phenomenon, and they have been reviewed by Kramer[16] and by Kramer and Berger.[17] Their findings have shown that the craze stress, which is normal to the craze plane, is linked to the entanglement density. The essence of Kramer's explanation is that for a craze to be stable molecular entanglements must exist. For an amorphous polymer of sufficiently high molecular weight, interactions that occur in the melt state are assumed to also occur in the craze state, as if it were a rubbery network. These make up the necessary entanglements for stable crazes. Typically a polymer with a high entanglement density will have a high crazing stress; such a polymer may deform more easily by yielding. It is not known what effects, if any, molecular motions detected as the secondary relaxation have on entanglements and therefore on the craze stress. We note that the work reviewed by Kramer[16] and by Kramer and Berger[17] focuses on craze growth and the process of transformation of crazes into cracks. They did not address the important issue of craze nucleation.

In this study, we examine these issues by investigating the properties of a series of amorphous, random copolyesters based on PET and poly(1,4-cyclohexylenedimethylene terephthalate) (PCT). The impetus of this study lies in the discovery of the shifts in the ductile−brittle transition temperature from Izod impact tests of the copolymers (on relatively thin, 3.2 mm thick specimens) to lower temperatures (Figure 1) as the copolymers become more PCT-like. This is an obvious case where a systematic change in the chemical structure has apparently facilitated the polymers' shear yielding process. The results of an in depth study of the molecular motions giving rise to the secondary relax-

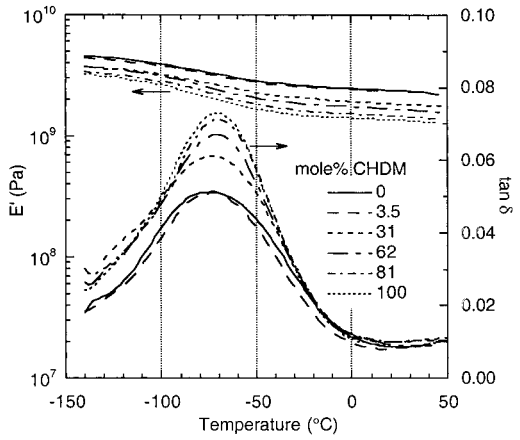

Figure 2. Secondary relaxation from dynamic mechanical spectroscopy of PET/PCT copolymers at 1.0 Hz

ations of these copolymers are described in a previous publication.[18] We briefly summarize some of the more pertinent findings here. The polyesters all exhibit a strong secondary mechanical loss peak near −70 °C at 1 Hz (Figure 2). The tan δ peaks increase in magnitude with only slight shifts in the peak temperature. For those containing the cyclohexylene linkage, the increase in the secondary relaxation peak was shown to involve conformational transitions of the cyclohexylene ring. By way of dipolar rotational spin-echo ^{13}C NMR, large-amplitude motions of the cyclohexylene rings in the copolyesters and PCT were detected. The rings are believed to undergo conformational transitions that can, when moving cooperatively with rings of adjacent repeat units, induce translational motions of the connecting terephthalate groups. The concerted motion may give rise to longer-ranged translational excursions along the chain. We believe these cooperative motions of the secondary relaxation play an important role in mechanical performance such as the ductile−brittle transition. The scope of this work is to further understand how molecular motions may influence such behavior, specifically in yielding and crazing. In the following we describe experiments on measuring the yield stress and its dependence on strain rate, the craze stress, and the amount of dynamic fluctuation in the glasses using positron annihilation lifetime spectroscopy.

Experimental Section

Materials. A series of random, amorphous copolyesters derived from dimethyl terephthalate and ethylene glycol and/or 1,4-cyclohexylene dimethanol (CHDM) were used in this study. The copolymers were based on PET with the following increasing mole percentages of the diol CHDM: 3.5, 31, 62, and 81 mol %. The PCT homopolymer had 100 mol % CHDM. The cyclohexylene rings in the copolyesters and in PCT had a trans-to-cis molar ratio of 68:32. The molecular weights of the polymers were determined by GPC as PET equivalents and are given in Table 1 of ref 18 along with the repeat unit structures. The materials were supplied by the Eastman Chemical Co. in the form of injection molded tensile bars and plaques and were confirmed as random copolymers by NMR results. All specimens tested were amorphous.

Positron Annihilation Lifetime Spectroscopy (PALS). PALS was performed using a radioactive source ($^{22}NaCl$) and the conventional fast timing technique at 25 °C. The PALS technique has been extensively described in recent literature[19] and will not be described here. However, it is useful to point out that orthopositronium (o-Ps) can localize in static nanopores (e.g., cagelike structures in some glasses and crystals) as well as in transient nanopores generated by molecular motion. Only the latter is of interest here. Distinguishing between static and thermally generated or dynamic components is possible by extending PALS measurements to low temperatures.[20] It was found that at room temperature most of the nanopores detectable by PALS for glassy polymers are "dynamic", i.e., due to thermally excited molecular motion. The remainder, which is determined by extrapolating the data to 0 K, is "static", i.e., due to the inherent packing defects in the glass. Since the lifetime of orthopositronium is too long (∼2 ns) to localize in molecular volume generated by high-frequency vibrations (< ps), the dynamic nanopores measured is largely due to the slower motions such as those detected in dynamic mechanical spectroscopy as secondary relaxation motions. When this technique is applied to materials such as the present series of copolymers, the nanopores detected at room temperature can be assumed to be dominated by local segmental motions, especially for the purpose of relative comparison. We further note that the differences in T_g in this series of copolymers is relatively small and is unlikely to contribute to any differences observed. Specimens for PALS were tested in the as-molded condition.

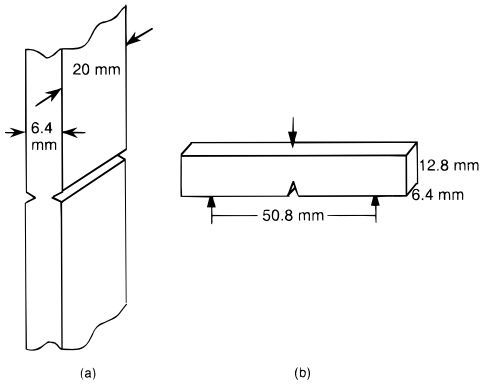

Figure 3. Schematic illustrations of notched specimens (ρ = 0.254 or 0.127 mm) used for craze testing in (a) uniaxial tension and (b) three-point bending.

Yield Tests. The temperature and strain rate dependencies of the yield stress were determined by performing a series of tensile tests on the copolyesters using a servohydraulic Instron testing machine (model 1331) equipped with a temperature chamber of ±1 °C stability. The injection molded tensile bars were used as-received. The strain in each tensile specimen was monitored using an extensometer (MTS model 632.11B-20) of 25.40 mm gauge length and 3.81 mm maximum travel and was tested at temperatures between −40 and 60 °C and at strain rates between 3.6×10^{-4} and 2.2×10^{-1} s^{-1}. The yield stresses were based on the original cross-sectional areas of the specimens and are therefore nominal stresses. The data are presented as plots of nominal yield stress vs log(strain rate) for the temperatures tested.

Crazing Tests. The craze stress was determined using specimens containing blunt notches. This was necessary because in simple tension the materials would simply yield. The blunt notches were used to produce a high level of hydrostatic tension arising from plastic constraint. The hydrostatic tension was what eventually produced the crazes. The magnitude of the hydrostatic tension was calculated using Hill's slip-line field theory.[21] Two modes of testing were used. The first was uniaxial tension and required rectangular specimens which were cut from 12.7 cm × 12.7 cm × 6.4 mm injection molded plaques. The rectangular bars were 20 mm × 6.4 mm in cross section and 127 mm in length. The gauge length of the specimen was nominally 70 mm. The bars were notched using a TMI notch cutter. V-notches of 0.254 mm or of 0.127 mm radius were introduced to opposite faces of the bar at a depth of 1.3 mm as shown in Figure 3a. To prevent plastic deformation at the notch tip induced by the cutting, cold N_2 gas was blown into the notch area during the machining process. The crazing tests were performed by pulling the bars in tension at a fairly high cross-head speed

of 254 mm/s. (At lower speeds the materials did not consistently craze.) All crazing tests were performed at room temperature. The fracture surfaces were examined using SEM (Hitachi S800) to determine the craze nucleation site. Two samples were tested per copolymer for each size of notch radius used.

The second mode of testing was three-point bending. Single edge notch bend specimens were cut from 12.7 cm × 12.7 cm × 6.4 mm injection molded plaques. Rectangular bars of 12.8 mm × 6.4 mm cross section and 63 mm in length were notched using a single point flycutter. V-notches of 0.254 or 0.127 mm radius were introduced through the thickness of the bars at a depth of 2.5 mm as shown in Figure 3b. The craze tests were performed in a falling weight Charpy geometry (i.e., three-point bend) at a speed of 1 m/s. Five samples were tested per copolymer for each size of notch radius used.

Results and Discussion

PALS Results. In parts a and b of Figure 4, τ_3 and I_3 are plotted as a function of increasing CHDM content, respectively. Values of τ_3 increase from 1.735 to 1.853 ns, which, assuming microscopic holes of spherical shape, correspond to average void radii of 2.543 to 2.659 Å. The total hole volume V_h can be computed from $V_h = C\nu_h I_3$ where C is a constant for a given polymer, and ν_h is the average hole volume calculated from the average hole radius. The hole volume fraction is defined by $F_h \equiv V_h/V$ where V is the total volume. To be able to compare the values of F_h for the copolyesters, we must first consider how C might change with the copolymer composition. The determination of C for glassy polymers has been discussed by Hristov et al.[20] Since the chemical makeup is similar between the various copolyesters studied, we assume C to be constant for the different copolyesters. The trend exhibited by the relative fractional hole volume F_h with increasing CHDM content is shown in Figure 4c. It can be seen that F_h increases by nearly 40% in going from PET to PCT.

The results shown in parts a and b of Figure 4 indicate that both the size and number of the holes increase with increasing CHDM content, respectively. By examining the trends of τ_3 and I_3 alone, it is not possible to determine whether the dynamic contribution dominates the increase in hole volume. The copolyesters contain trans and cis cyclohexylene rings at a molar ratio of 68:32. Thus, we expect an increase in open volume from the less efficient packing due to the presence of the cis isomers. However, this contribution is expected to be small. On the other hand, DMS and NMR results indicate that the cyclohexylene rings do add long-range cooperative chain mobility to the copolyesters, perhaps through translational movements of the chain segments.[18] Since these motions continue to be active below T_g, they contribute to the open volume by their movements. These results suggest that dynamic fluctuations are responsible for the majority of the hole volume detected and are increasing as greater numbers of cyclohexylene groups are introduced into the polyester backbone. This supports the notion that the cyclohexylene group increases molecular motion of the polymer chain.[18] We shall attempt to show in the following that the enhanced dynamic fluctuation has a significant effect on the mechanical properties of these polymers.

Yield Stress Results. The temperature and strain-rate dependence of the yield stress of PET, the copolymers with 31 and 62 mol % CHDM, and PCT are plotted in Figure 5a−d, respectively. It can be seen plainly from the straight lines drawn through the isothermal data in the plots that, at the lowest and highest temperatures

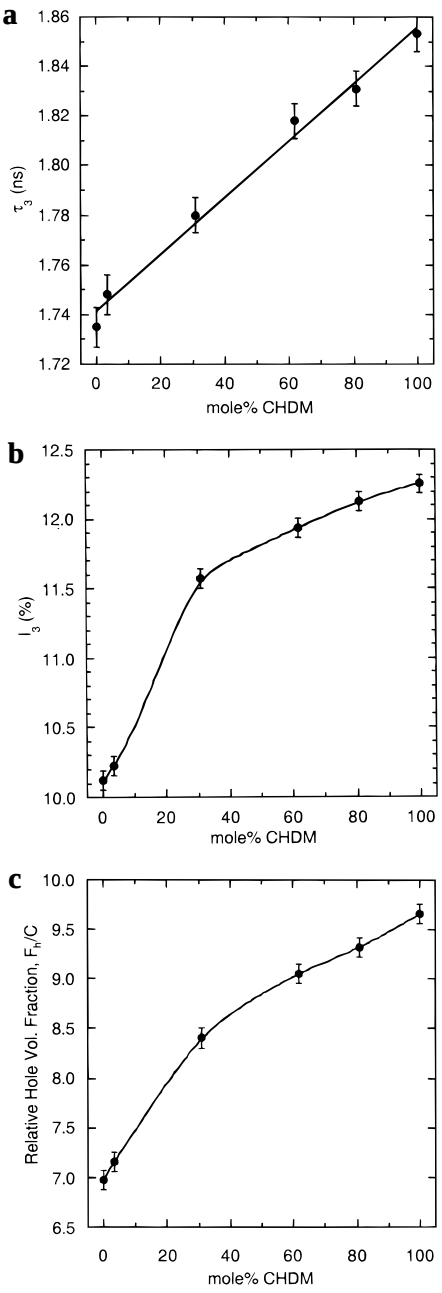

Figure 4. (a) Change in τ_3 with increasing CHDM content (T = 25 °C). (b) Change in I_3 with increasing CHDM content (T = 25 °C). (c) Change in relative hole volume fraction with increasing CHDM content (T = 25 °C).

tested, the yield stress has a greater dependence on the strain rate than at the intermediate temperatures. The observation regarding the lower test temperatures (−40 to 0 °C) can be attributed to the effects of the secondary relaxation detectable by dynamic mechanical tests. However, at the highest temperature (60 °C), the increase in strain-rate dependence of the yield stress is counterintuitive. We will first discuss how the secondary relaxation can influence the strain-rate dependence of the yield stress followed by possible explanations for the high-temperature observation.

Before any direct comparison between tensile yield data and dynamic mechanical results can be made, the difference between the strain rate used in yield tests and the frequency in the dynamic mechanical tests must first be addressed. A relationship between strain rates of tensile tests and frequencies of dynamic mechanical

Table 1. Equivalent Frequencies for the Strain Rates in Tensile Tests

crosshead speed (in./min)	strain rate (s^{-1})	equiv freq (Hz)
0.1	3.6×10^{-4}	0.09
1	3.6×10^{-3}	0.8
2	7.2×10^{-3}	1.6
3.2	1.1×10^{-2}	2.4
10	3.6×10^{-2}	8.0
60	2.2×10^{-1}	49

tests must be established if we wish to determine how the tensile yield behavior is affected by the participation of the secondary relaxation. For a motion to contribute to macroscopic deformation behavior, it must be available at a given strain rate and temperature. Dynamic mechanical tests probe the molecular motions which are thermally activated at the test temperature. If the strain rate of the tensile test is comparable to the frequency of the dynamic mechanical test, then one can determine whether the molecular motion detected by dynamic mechanical tests is available at the start of the tensile test at a given temperature. Although the overall strain regimes are totally different for the two tests, strain rates at the very beginning of each test may be compared since they are still within the elastic regime for both tests. Since the amplitude of the strain used in dynamic mechanical tests was kept constant (0.113%), an equivalent frequency can be determined for the tensile yield strain rate as if it were to behave sinusoidally with time. This method of frequency equivalence was used by Xiao et al.,[8] and we follow a similar procedure here. At a tensile strain rate of 7.2×10^{-3} s^{-1}, an equivalent frequency of 1.6 Hz can be approximated. Equivalent frequencies of all the tensile yield strain rates are given in Table 1. Although this is a very rough estimate, and should be confined to very small strains, one can infer that if a molecular motion detected by dynamic mechanical tests at 10 Hz and 0.113% amplitude were available at room temperature, that same motion should also be available in a tensile test at 3.6×10^{-2} s^{-1} at room temperature.

The equivalent frequencies corresponding to the tensile strain rates overlap well with the 0.3−30 Hz frequency range used in previous dynamic mechanical tests.[18] The tan δ loss peaks of our dynamic mechanical results indicate that the secondary relaxation is not completely activated until at temperatures of at least 20 °C for the frequencies used. (The peaks have a full width at half-maximum of 75−85 K.) Therefore, motions of the secondary relaxation are not completely available in tensile yield tests at equivalent strain rates until temperatures above 20 °C. This explains the change in strain rate dependence of the yield stress as the testing temperature is increased from −40 to 0 °C. The strain-rate dependence of the 25 and 40 °C yield stress curves appear fairly constant (Figure 5a−d). At these temperatures, the thermal activation of the secondary relaxation is complete.

Next we offer a possible explanation for the increase in strain-rate dependence for the 60 °C isotherms. Allison and Ward have shown that the yield stress of PET decreases linearly with increasing temperature and that an abrupt change in the slope of the curve occurs as the glass transition is approached[22] as represented by curve A in Figure 6. This has been shown for other polymers as well.[23,24] The change in slope occurs at a temperature which we will refer to in Figure 6 as T_{gyield}. At a strain rate higher than that used in curve A, the yield stress at T_{gyield} will be higher than that given by curve A. In other words, at higher strain rates, the material is effectively further away from T_{gyield} and therefore behaves as if it were at temperatures below T_{gyield}; this is illustrated by curve B. On the other hand, at strain rates lower than that of curve A, the yield stress at T_{gyield} will be lower and will behave as if it were above T_{gyield}, as indicated by curve C. One notes that the strain-rate dependence of the yield stress above T_{gyield} is much greater than below T_{gyield}. Similarly, we propose that at these lower strain rates an effect similar to curve C is taking place, thereby decreasing the yield stress more than expected and giving the 60 °C isotherms the appearance of a higher strain-rate dependence. The fact that this effect is most prominent for PET (Figure 5a) and least noticeable for PCT (Figure 5d) is supportive of our explanation. The T_g's for PET and PCT are 72 and 96 °C, respectively, by DSC.

Activation Energy and Volume for Yielding from the Eyring Model. According to Eyring's model in eq 1, given in the Introduction, plots of the temperature-normalized yield stress against the logarithm of the strain rate should give a series of parallel linear isotherms from which the activation energy and volume can be determined. However, at the temperatures tested for the PET/PCT copolymers, the plots (Figure 5a−d) do not result in parallel isotherms. In previous studies, the yield stress for polycarbonate[12] and other polymers including PMMA[13] and PVC[12] has shown similar results. The yield stress has been shown to increase more rapidly with increasing strain rate and decreasing temperature at low temperatures and high strain rates than at high temperatures and low strain rates. In these cases, the Eyring model was applicable over very wide ranges of strain rates and temperatures only if the model was revised to incorporate two activated rate processes acting in parallel. This modification of the Eyring model gave a better fit to experimental data and was used to support the assertion that a quantitative link exists between the second process and the dynamic mechanical secondary relaxation.[13−15] The ΔH of the second process was compared to the activation energy of the secondary relaxation. If the two were of similar magnitude, it was then thought to confirm that the second process involved the secondary relaxation. The fundamental difficulty with this conclusion, and the reason why we do not use a similar treatment here, is the assumption that the two processes can be linearly combined. On the basis of the nature of the secondary relaxation, i.e., one consisting of cooperative motions of chain segments, one expects coupling, i.e., interactions between neighboring chains, leading to nonlinearity in the activation of segmental motions. For these reasons, we are careful to apply Eyring's model only to the 25 and 40 °C isotherms of the yield data. In these temperature regimes, the secondary relaxation motion is fully activated and occurring at high frequency. Such temperatures are still well below the onset of the glass transition, so the primary relaxation motions are not accessible at our time scale. These yield stress isotherms are shown in Figure 7 for PET, the 31 and 62 mol % CHDM copolymer, and PCT. The data for PET are consistent with those published by Foot et al.[15] Their research covered a much wider range of strain rates (10^{-5}−10^{2} s^{-1}) and observed the characteristic bend in the yield stress curves at high strain rates (>1 s^{-1}) for

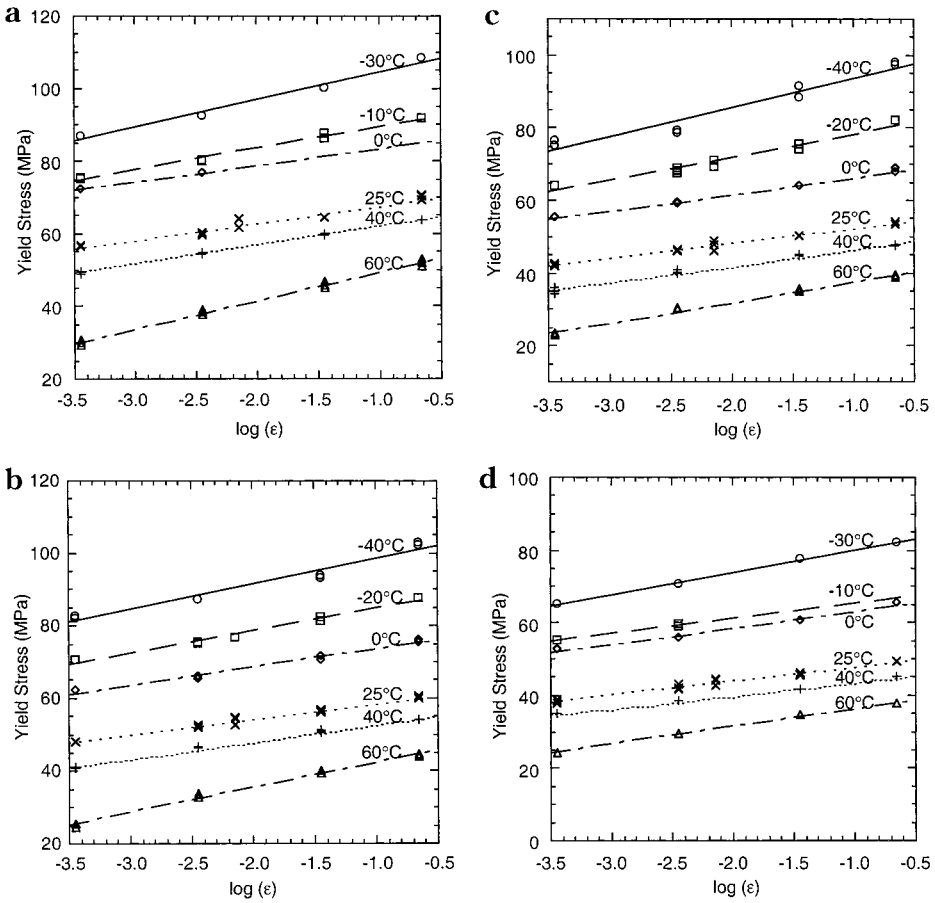

Figure 5. (a) Temperature and strain-rate dependence of yield stress for PET. (b**)** Temperature and strain-rate dependence of yield stress for 31 mol % CHDM copolymer. (c) Temperature and strain-rate dependence of yield stress for 62 mol % CHDM copolymer. (d) Temperature and strain-rate dependence of yield stress for PCT.

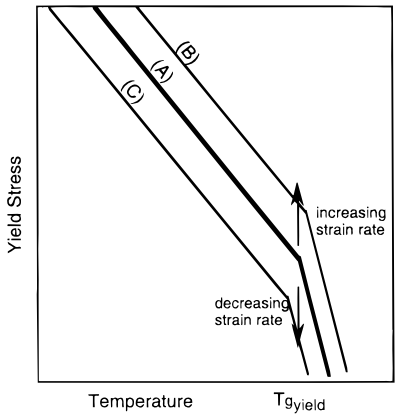

Figure 6. Variation of the yield stress with temperature for PET. The temperature dependence at a higher strain rate than that used in curve A is depicted by curve B and the lower strain rate by curve C; at higher strain rates the material is effectively further away from its T_{gyield} and behaves as if it were at temperatures below T_{gyield} ; at lower strain rates, the yield stress at T_{gyield} will be lower than that measured in curve A and behaves as if the temperature were above T_{gyield}.

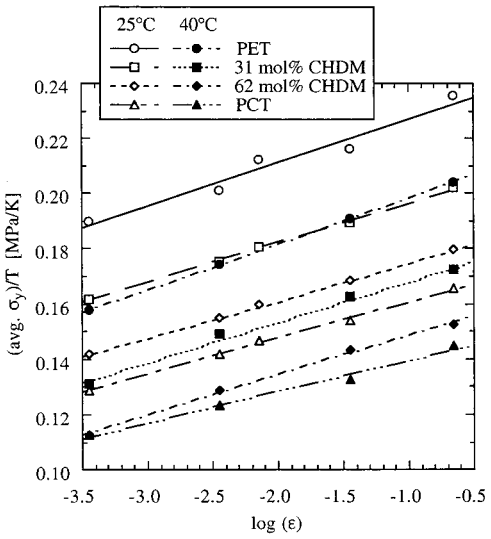

Figure 7. Strain-rate dependence of the average yield stress normalized by temperature for PCT, 31 and 62 mol % CHDM copolymers, and PCT at 25 and 40 °C.

higher testing temperatures. They fit Eyring's model as two activated rate processes to their data to calculate the activation energy and volume. Because we are certain that at 25 and 40 °C only the motions of the secondary relaxation are active for the strain rates used in our yield tests, we assume a single process and fit eq 2 to our data. The 25 and 40 °C curves, which are parallel, were used to find the activation energies and volumes. The activation energies ΔH are shown in Table 2 and range from 49 to 54 kcal/mol without any distinct trend with respect to the composition. The activation energy for PET compares well with the 45 kcal/mol found by Foot et al.

The activation volume ν, however, exhibits a distinct trend as the CHDM content increases (Table 2). It increases from 1.95 nm^3 for PET to 2.63 nm^3 for PCT between 25 and 40 °C, an increase of 35%. Foot et al. found a smaller value of ν for PET,[15] viz., 1.21 nm^3. We

Table 2. Activation Energy and Volume of Yielding Calculated from Eyring's Model and Specific Volume at 25 °C

mol % CHDM	E_a (kcal/mol)	V (nm^3)	specific vol (cm^3/g)
0 (PET)	49.2	1.95	0.74
3.5	52.4	1.97	0.78
31	53.7	2.19	0.80
62	51.8	2.27	0.81
81	50.4	2.38	0.83
100 (PCT)	53.7	2.63	0.85

see that for similar activation energies PCT has a larger activation volume than PET. For comparison, we also show in Table 2 the specific volume of the polymers at 25 °C. These data show that the specific volume of PCT is only about 10% larger than that of PET. Thus, the increase of activation volume is not due to the molecular volume alone. At this point we recall Eyring's definition of the activation volume. It was defined as the volume swept out by the chain or chain segment during molecular flow over a potential energy barrier. More specifically, it was given as the product of the cross section of the moving segment and the distance traveled by that segment. Researchers have attempted to correlate this volume with the scale of molecular motion of the secondary relaxation. Using this technique, the activation volumes for several amorphous polymers with various thermal histories were compared.[24−27] Different values of the activation volume were found which seem to primarily stem from the different forms of the Eyring flow equation used and the different experimental conditions under which the data were obtained. More importantly, however, the physical meaning of the activation volume itself must be understood. Although it has been suggested that this volume may correlate to the scale of motion of the secondary relaxation, it actually groups all possible chain displacements into a single parameter. In other words, the Eyring model assumes that the movement of the molecules defined by the activation volume and energy accounts for all the strain imposed on the system. Therefore, it could encompasses a volume more extensive than motions of the secondary relaxation alone.

With this understanding, comparison of activation volumes of different polymers is still useful, however, given that the experimental conditions used for all the polymers are similar. The activation volume can be considered an indicator to the scale of molecular motion at yielding. In this manner, the activation volume is an important parameter to monitor, although it is difficult to assign the activation volume to a specific molecular motion. Here, the activation volume of the polyesters increase significantly as the polymers become more PCT-like despite their similar activation energies. We believe this to be due in part to the motions of the secondary relaxation, which will be discussed further in the proceeding section.

The Effect of Molecular Fluctuations on Yielding. We present in this section a hypothesis on the effect of molecular motions and the resulting fluctuations on the ability of the polymers studied to yield. For the copolymers containing the cyclohexylene linkage, the secondary relaxation was shown to involve conformational transitions of the cyclohexylene ring.[18] Dipolar rotational spin-echo ^{13}C NMR detected large-amplitude motions of the carbons in the 2, 3, 5, and 6 positions with respect to the carbons in the 1 and 4 positions in the cyclohexylene rings in the copolyesters and PCT. The rings are therefore shown to undergo conformational transitions (chair−boat−chair) that can, when moving in concert with rings of adjacent repeat units, induce translational motions of the connecting terephthalate groups. The concerted motion may give rise to longer ranged translational excursions along the chain. Such motions create dynamic, fluctuating volume, as found by PALS. The effect of activation of these motions is to reduce interactions between chains and thereby reduce the resistance for chains to slide relative to one another when an external stress is applied. This effect can be likened to lubrication on a molecular level. By facilitating lateral slipping of chain segments, large-scale sliding of chains is feasible, thus increasing the activation volume. Macroscopically, the yield stress is reduced, and the ductility is enhanced. We emphasize that molecular motions beneficial to yielding are those that are capable of creating dynamic fluctuation. For example, poly(cyclohexyl methacrylate) (PCHMA) has a large, narrow secondary loss peak which has been shown indisputably to be due to the cyclohexyl substituent on the side chain.[28,29] However, PCHMA is brittle at temperatures well above its secondary relaxation. The motion of the cyclohexyl group in this case is only weakly coupled to the main chain and probably cannot give rise to significant dynamic fluctuation in the material.

The lower yield stress of PCT relative to PET supports the assertion regarding the effect of fluctuations described above. At the temperatures used to determine ΔH and ν, namely 25 and 40 °C, the secondary relaxations of all the PET/PCT polymers are thermally activated. The cyclohexylene groups increase dynamic volume fluctuations by inducing translational excursions along the chain. Depending on the configuration of the segments between the cyclohexylene groups, these excursions could have stronger transverse or axial components. Thus, as the population of cyclohexylene groups increases, the amount of fluctuation throughout the material increases. Likewise, as the number of mobile chain segments increases, stress activation causes an even larger number of segments to participate in the yield process. The reduction in yield stress by these translational motions is not simply a concentration effect alone. The size of these excursions must also be taken into consideration. Xiao et al. have shown, for example, that as the size of the Bisphenol A carbonate block in B_xtT_x increases (B = Bisphenol A carbonate, t = terephthalate linkage, T = tetramethyl-Bisphenol A carbonate, x = number of units in a block), the yield stress decreases.[8] Their explanation for this phenomenon relies on the existence of motional cooperativity in the B blocks. As the block length increases, the scale of in-chain cooperative motion increases, making the stress activation even more efficient at inducing yielding. In other words, increased volume fluctuation from motions that incorporate several repeat units cooperatively are likely to be more proficient at "lubricating" the system.

The notion that cooperativity enhances ductility can also be projected onto this PET/PCT series. It is suggested in a previous publication[18] that an in-chain cooperative relaxation exists for PCT. We expect that for this polymer the cyclohexylene ring moves in a concerted fashion with the cyclohexylene ring of the neighboring repeat unit. Thus, for PCT the correlation length is a single repeat unit. However, as the cyclo-

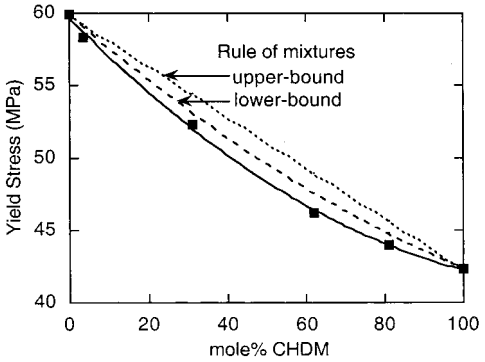

Figure 8. CHDM concentration dependence of yield stress (25 °C, 3.6×10^{-3} s^{-1}); dotted lines are based on the rule of mixtures.

hexylene content is decreased, that is, as the mole percent of CHDM is reduced, the correlation length could increase. This would lengthen the scale of cooperativity along the chain. The effect of enhanced in-chain cooperativity on yielding can be seen in Figure 8. Had the yield stress been determined solely by the CHDM concentration, the yield stress of the copolymers might have been expected to follow closely the rule of mixtures using the yield stresses of the homopolymers (PET and PCT). Both the upper-bound and lower-bound values determined by the rule of mixtures are depicted in Figure 8. However, copolymers with 31 and 62 mol % CHDM exhibit yield stresses even lower than those predicted by the lower-bound rule of mixtures. Although we do not know the correlation length of the local motion in the copolymers, we postulate that enhanced cooperativity further facilitates yielding. At more dilute levels of CHDM, the cooperative advantage is overwhelmed by the energy required to translate extensive segments of the chain. The motions of the cyclohexylene groups are dampened by the many repeat units separating each ring such that one ring can no longer benefit from the movement of its neighboring ring. This is consistent with our solid-state ^{13}C NMR results.[18] The copolymers with higher CHDM content generally had higher mobility for the doubly protonated carbons of the cyclohexylene ring than the copolymers of lower CHDM content. This indicates that the cyclohexylene ring of PCT-like copolymers are more likely to undergo the chair−boat−chair motion than those of the PET-like copolymers.

Having discussed ductile behavior in the polyester series, we investigate brittle failure in the next section. This is done by investigating how the craze stress changes as the cyclohexylene ring concentration is increased.

Craze Stress Results. In this study of the craze stress, PET and PCT homopolymers could not be used because of the difficulty in molding thick yet amorphous specimens. In both cases, the development of crystallinity during molding was a problem evidenced by the opaque appearance of the specimens. Ultimately, only the copolymers were used. The craze stress, σ_{cr}, was determined using Hill's slip-line field theory which determines the hydrostatic stress in the plane strain yielded zone.[21] The dilational stress produced by the stress triaxiality at the elastic−plastic boundary is responsible for craze and fracture initiation, which we designate as σ_{cr}. It is calculated by the following equation:

$$\sigma_{cr} = \sigma_p = \tau\left[1 + 2\ln\left(1 + \frac{s}{\rho}\right)\right] \qquad (2)$$

where τ is the shear yield stress, s the distance from the notch tip to the craze nucleation site, and ρ the notch tip radius. The shear yield stress τ can be calculated from the uniaxial yield stress by assuming that the yield criterion of the polymer obeys the von Mises yield criterion, viz., $\tau = \sigma_y/\sqrt{3}$. The yield stress, σ_y, and the crazing stress must be determined at comparable strain rates. In principle, eq 2 is valid only for elastic−perfectly plastic materials. However, Ishikawa et al. found it to be applicable to certain plastics including polycarbonate,[30] which is quite similar to the materials studied here. The strain rate when crazing occurred was estimated by followed the guidelines of Ishikawa et al. which state that the maximum principal strain at the notch tip is about 6 times the yield strain when the plastic zone size reaches its maximum.[30] Although the craze nucleation site was a small distance away from the notch tip, we assumed that the strain at the nucleation site was 6 times greater than the far field strain as a worse case scenario. Thus, the strain rate at the crazing site is assumed to be 6 times the average strain rate. Values of yield stress at this strain rate were found by using σ_y vs log(strain rate) master curves obtained from time−temperature superposition of yield stress isotherms. Studies of plane strain fracture of notched, amorphous polymers using Hill's slip-line field theory are well documented,[31−33] demonstrating this convenient method of determining σ_{cr}.

The craze stresses for the copolymers are given in Table 3 and are shown to increase as the CHDM content increases. It became increasingly difficult to induce crazing and brittle failure in the uniaxial tension tests of the PCT-like specimens at room temperature. Indeed, the copolymer with 81 mol % CHDM always exhibited ductile failure even when a relatively sharp notch radius of 25 μm (0.001 in.) was used. The stresses calculated from the uniaxial tensile tests agree well with those found from three-point bending tests despite the difference in strain rates. The strain-rate insensitivity of the craze stress has been shown for other glassy polymers[34] and is now considered to be a characteristic of the craze stress. The same researchers also showed that the temperature dependence is much greater for the shear yield stress than the critical hydrostatic stress.[30] The

Table 3. Craze Stress and Associated Experimental Parameters

mol % CHDM	3.5	3.5	31	31	62	62	81	81
notch radius	0.254	0.127	0.254	0.127	0.254	0.127	0.254	0.127
uniaxial tension								
plastic zone size	104	51	209	98	D[a]	151	D	D
	76	75	89	88		94		
3-point bending								
plastic zone size	120		240		310	180	440	240
σ_{cr} (MPa)	78		90		92	98	102	106

[a] "D" indicates ductile failure (bars with 0.064 and 0.025 mm notch radii were also tested but also resulted in ductile failure).

plastic zone size, i.e., the distance between the craze nucleation site and the notch tip, *s*, can be accurately measured by pinpointing the craze nucleation site on the fracture surface using an SEM. The nucleation site is generally located in the smooth flat zone where fracture proceeds relatively slowly. The distance *s* of eq 2 is equivalent to the extent the plastic zone has grown from the notch tip prior to failure. From Table 3 we see that as the CHDM content increases, the size of the plastic zone, *s*, also increases. Ishikawa et al. observed an increase in the plastic zone size as the testing temperature increased for several glassy polymers.[30] In fact, by extrapolating back to the point where the fracture nuclei coincides with the notch surface, i.e., where $s = 0$, they found that the temperature approximated the secondary relaxation temperature. Hence, they attributed the increase in *s* at higher temperatures to the availability of motions of the secondary relaxation.

For the copolyesters, the increase in plastic zone size with increasing cyclohexylene concentration is effectively equivalent to an increase in temperature. The molecular motion provided by the cyclohexylene group at room temperature acts as if it is an internal lubricant, facilitating chain sliding and yielding and consequently the growth of the plastic zone. In this manner, these motions not only help relieve the external stress by creating a plastic zone but also prevent the triaxial stress from escalating toward the level of the critical stress for crazing. Therefore, the greater the effectiveness of the molecular motion as an "internal lubricant", the more likely the material will escape brittle failure. In fact, in Hill's theory a maximum hydrostatic stress is obtained when the plastic zone reaches the maximum extent of the logarithmic slip-line field, *s**. When $s \geq s$, the triaxial stress achieves its maximum value and no longer continues to increase. The maximum extent of the logarithmic slip-line field, *s**, is defined by the geometry of the notch as

$$s^* = \rho\left[\exp\left(\frac{\pi}{2} - \frac{\omega}{2}\right) - 1\right] \tag{3}$$

where ρ is the radius of the notch and ω the notch angle. For the specimens used $\omega = 45°$, $s^*(\rho = 0.010$ in.$) = 570\ \mu$m, and $s^*(\rho = 0.005$ in.$) = 285\ \mu$m. Substituting *s** for *s* in eq 2, the maximum attainable hydrostatic stress $\sigma_{p,max}$ for each copolyester can be calculated. If $\sigma_{cr} > \sigma_{p,max}$, then ductile failure will ensue, and the plastic zone at the notch tip will simply continue to grow through the entire sample forming a so-called "plastic hinge". As an example, for the 31 mol % CHDM copolymer, at the high strain rate used, ($\sigma_{cr} = 90$ MPa) < ($\sigma_{p,max} = 135$ MPa); consequently, brittle failure by crazing ensues. On the other hand, for the 81 mol % copolymer, σ_{cr} approaches $\sigma_{p,max}$ such that ductile failure becomes much more probable.

The Effect of Molecular Fluctuations on Craze Initiation. We present in this section a hypothesis on the effect of molecular motions and the resulting fluctuations on the tendency of the polymers studied to craze. It is evident that for ductile deformation high σ_{cr} and low σ_y are desired. This means increasing σ_{cr} by modification of the polymer's chemical structure must not be at the expense of the ability of the polymer to yield. This prescription is satisfied by the copolyesters studied here. In Figure 9, σ_{cr} and σ_y are plotted as a function of CHDM content. As σ_y decreases, σ_{cr} increases

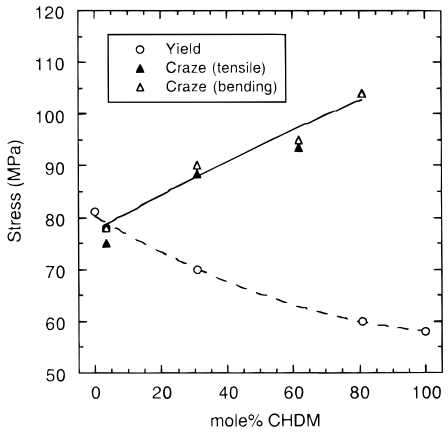

Figure 9. Yield and craze stress as a function of CHDM content determined at $\dot{\epsilon}$ of approximately 22 s^{-1} and room temperature.

with increasing cyclohexylene concentration. The σ_{cr} increase can be understood by examining factors that influence craze initiation. These include thermal history, molecular weight, and entanglement density.[35] The first two of these parameters are quite similar for each of the copolymers. Since the samples were prepared by very similar molding conditions and are of comparable molecular weights (Table 1 of ref 18), we do not expect the increase in to be due to these factors. In addition, it has been shown that the crazing stress has no molecular weight dependence as long as the molecular weight is much greater than twice the entanglement molecular weight,[36] i.e., $M_n \gg 2M_e$. (This implies that craze initiation is not accompanied by large-scale segmental motions.) Even physical aging concerns can be disregarded due to the similarity in thermal history.

The significance of the entanglement density can be assessed by understanding that craze initiation results from cavitation due to a dilative stress component imposed on the heterogeneous, glassy structure.[37−39] Argon and Hannoosh regarded craze initiation as the creation of microvoids, possibly due to the scission of chains. Furthermore, they viewed cavitation as a stress-dependent kinetic process whereby the number of microvoids increased with time. Eventually the microvoids are proposed to plastically expand and transform into craze nuclei.

A similar but simpler approach is given by Kausch.[40] Similar to the picture given above of a glassy polymer containing molecular heterogeneity, this proposal, however, does not presume the preexistence of plastic deformation. According to Kausch, an elastically strained region will have areas of locally lower chain density. Unstable microvoids form in these regions from decohesion due to the dilative stress. In an adjacent region where the chain density is sufficient to inhibit decohesion, anelastic deformation of this area takes place, the strain is transferred from the initial region to these adjacent regions, and the microvoids become stabilized. This process continues with sustained or increased loads such that the microvoids coalesce, leaving fibrils that connect the opposite craze surfaces.

From these descriptions of craze initiation, polymers of low entanglement density are expected to undergo microvoid formation at lower stresses. The entanglement density ν_e is proportional to the bulk density and inversely proportional to the entanglement molecular weight which can be found from the rubbery plateau

modulus.[16,17] However, in the case of the copolyesters, crystallization occurs at temperatures above T_g, rendering attempts to measure the plateau modulus futile. For this reason we use van Krevelen's method for estimating the entanglement molecular weight.[41] It is expected to increase as more cyclohexylene groups are added to the backbone. The decrease in density also adds to the expectation of a decreasing ν_e. By this argument, PCT should have fewer entanglements per unit volume than PET and should craze more easily. Contrary to this expectation, the crazing stress is found to be much higher for PCT than for PET. A possible interpretation of these seemingly contradictory results is to consider the increasing molecular motion as the CHDM content is increased. Such local chain fluctuations can collapse nascent nanovoids and, thus, influence the craze initiation step described in Argon's and Kaush's craze nucleation process which are essentially quasi-static models. The stability of these voids is also key to the craze initiation process described by Hristov et al.[42,43] where transient voids several nanometers in diameter were detected in bulk polycarbonate during fatigue experiments. These voids collapsed when the fatigue stress was removed. They found that these voids, which should be called nanovoids, eventually coalesce to form stable craze nuclei several tens of nanometers in diameter when the stress amplitude or the number of fatigue cycles became high enough. In a region of low entanglement density where nanovoids are most likely to form, motions of those parts of the molecules in this area can allow for sufficient relaxation of the nanovoids such that points of low density never fully mature into stable nanovoids. The material is able to maintain a more uniform stress distribution, and craze nucleation is thwarted. In this way, any void localization remains unstable and gets "reabsorbed". This continues until the hydrostatic tension is high enough such that molecular redistributions are no longer able to collapse the voids. At this point the nanovoid becomes stabilized along with other neighboring nanovoids, and together they proceed to form a stable craze.

This process can also be illustrated by a void nucleation theory. For a given volume of material, the introduction of a void will change the free energy of the system by some amount ΔG which is be given by

$$\Delta G = -\frac{4}{3}\pi r^3 B_{\text{strain}} + 4\pi r^2 \gamma_s \qquad (4)$$

for a spherical void of radius r. Here B_{strain} is a bulk strain energy term which decreases as r^3, and γ_s is a surface energy term which increases as r^2. This is illustrated in Figure 10. It can be seen that for a given applied hydrostatic tensile stress there is a critical radius, r^*, which is associated with a maximum excess free energy. If $r < r^*$, then the system can lower its free energy by collapsing the void. Thus, voids of $r < r^*$ are unstable. Voids can be stable if $r > r^*$. A nascent void may fluctuate just below r^* if the stress and thermal energy have the right magnitude. The fluctuation is caused by local segmental motion which is superimposed on the density fluctuation typical of all glasses. The larger the scale of molecular motion, the greater the fluctuation and the more unstable the void becomes as long as $r > r^*$. Since the dynamic fluctuation has a characteristic time scale, it is effective for relaxing the stress only if the strain rate is low compared to the relaxation time. When this condition is satisfied, the stress necessary to form a stable nucleus is increased. PCT has more fluctuation than PET, and thus craze nuclei are more unstable. The rate of strain energy decrease is proportionate to stress. Low levels of hydrostatic tensile stress increase the value of r^*. This shows that at low stresses or if the stress is rapidly relaxed r^* can become very large.

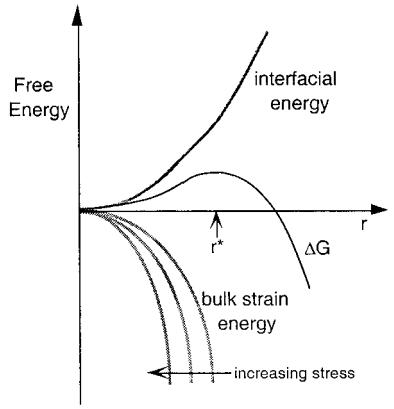

Figure 10. Schematic illustration of the free energy change associated craze initiation (homogeneous nucleation of a void of radius r).

Once crazes have nucleated, their widening depends on drawing of the craze fibrils to longer extensions. This can be accomplished by either disentanglement of the chain molecules or by chain scission. Because of the high strain rate used to determine the craze stress, the crazes may very well grow by chain scission. This process and the factors influencing it have been well documented by Kramer et al.[16,17] He and his associates developed a relationship for the craze widening stress S such that $S \propto \sqrt{\sigma_f \Gamma}$ where σ_f is the flow stress or drawing stress to propagate the neck after yield, and Γ is the craze surface tension. The latter parameter is further specified as $\Gamma = \gamma + {}^1/_4 \nu_e d_e U$ where γ is the van der Waals surface energy, ν_e the entanglement density, d_e is the rms end-to-end distance between entanglement points which is related to the entanglement molecular weight by $d_e \propto \sqrt{M_e}$, and U is the polymer backbone bond energy. For chain scission, then, $S \propto \sqrt{\sigma_f \rho}/\sqrt[4]{M_e}$. As the CHDM content increases in the copolyesters, σ_f has been shown to increase. The density ρ, however, decreases with increasing CHDM content ($\rho_{PET} = 1.35$ g/cm^3; $\rho_{PCT} = 1.21$ g/cm^3). Although M_e is expected to increase with CHDM content, its effect on the craze widening stress is reduced to the $-{}^1/_4$ power. Without further experiments, it is difficult to determine whether craze fibril extension will be facilitated or not by the addition of cyclohexylene rings. A decrease in the area of the slow-fracture (mirror) zone surrounding the craze nucleation site was observed for the three-point-bend samples, although no such trend was observed in the uniaxial tension specimens. This may indicate less craze stability in the PCT-like copolymers compared to the case of PET.

The Ductile/Brittle Transition and Toughening. Finally, the effect of the secondary relaxation on yielding and crazing can be used to explain the observed ductile–brittle transition of Figure 1. We see that as the CHDM content increases, the copolymer is able to exhibit ductile failure at lower temperatures. The molecular motions that facilitate yielding and delay crazing are more effective at high concentrations of CHDM as depicted in Figure 9. An alternate way of representing

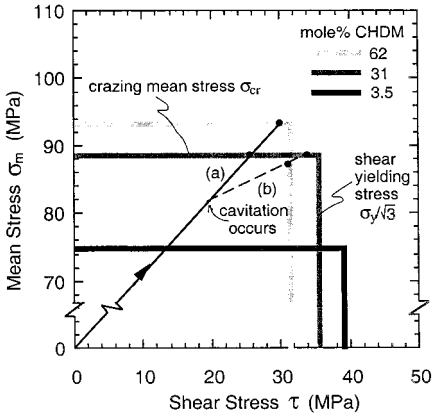

Figure 11. Schematic illustration depicting toughening effectiveness for an impact modifier. Path a: without rubber modification the stress state increases, and all copolymers show craze. Path b: with rubber modification, the stress state changes direction after cavitation enough to allow 62 mol % CHDM copolymer to shear yield.

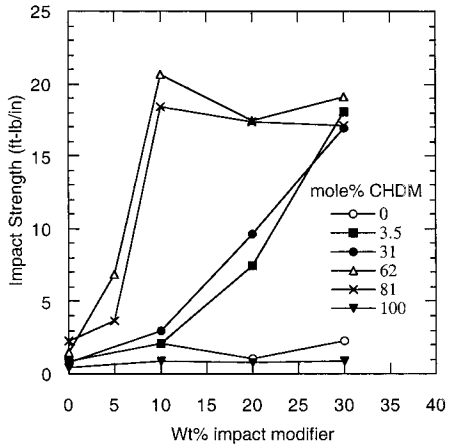

Figure 12. Notched Izod impact strengths of copolyesters blended with varying weight percent of EGMA impact modifier and tested at 0 °C; both homopolymers crystallize from rubber modification and exhibit brittle behavior.

the data in Figure 9 is shown in Figure 11 where the mean dilative stress σ_m is plotted against shear stress τ. The stress response of the copolymers is represented by envelopes in which the critical stress for crazing σ_{cr} comprises the upper (horizontal) boundary and the shear stress for yielding comprises the right (vertical) boundary for each envelope. In this plot the sensitivity of the shear yield stress to the mean stress is assumed to be zero, although in reality there is probably a slight dependence. In this manner, changes to the boundaries are more easily visualized. The upper boundaries (σ_{cr}) are more sensitive to CHDM content than the right boundaries (σ_y). Also, as the stress level is increased, it is possible to determine the likely outcome (crazing or yielding). This is especially useful for examining the effectiveness of rubber toughening. For example, Figure 11 shows the stress direction for a given stress state which combines a mean (hydrostatic tensile) stress and a shear stress. Such combinations are typical of stress states at a notch tip when the notch is opened by a stress. If the stress is allowed to continue to increase at the ratio depicted, the stress state would ultimately reach the upper boundary (σ_{cr}) for both the 31 and 62 mol % CHDM copolymers as indicated by path a. Crazing would then be the cause of failure for both copolymers. However, if the material contains a particulate impact modifier, cavitation of the modifier particles, when the critical stress level for cavitation is reached, changes the stress state of the material and the stress direction in favor of the shear stress component.[44] In other words, the ratio of the hydrostatic stress to the shear stress is reduced. A continued increase in the stress after cavitation, path b, still results in crazing for the 31 mol % CHDM copolymer but now results in yielding for the 62 mol % CHDM copolymer. In the latter case, the modifier is successful at toughening the system. In the former case, the behavior is still brittle and the impact modifier is ineffective. This was indeed the case as demonstrated by Figure 12. At 10 wt % EGMA (ethylene glycidyl methacrylate), the 0 °C notched Izod impact strength of the 62 mol % CHDM copolymer was significantly enhanced compared to that of the 31 mol % CHDM copolymer. To achieve a similar impact strength, the latter required rubber concentrations near 30 wt % EGMA. Clearly, such a high rubber content would have undesirable effects on other properties (e.g., modulus). As a side note, the rubber addition to PET and PCT induced crystallinity and resulted in brittle behavior.

The failure envelopes in Figure 11 were determined for an initial strain rate of 22 s^{-1}. Generally, σ_{cr} is not as sensitive to changes in strain rate as σ_y. Consequently for lower strain rates, the right boundaries would shift to the left, making yielding more probable. The same is expected for an increase in temperature. These envelopes then are useful in predicting the ductile/brittle transition temperatures for a given strain rate and a given stress state. In addition, the failure envelopes can give a complete map of the expected toughening efficacy for a given polymer−modifier system.

Conclusions

It has been shown by PALS that the volume fraction of nanopores increases significantly with the cyclohexylene content. These nanopores are most likely dynamic in origin. It has also been shown that the yield stress of the PET/PCT series of amorphous, random copolymers decreases as the cyclohexylene content increases. This holds for temperatures ranging from −40 to 60 °C and strain rates from 0.00036 to 0.22 s^{-1}. The decrease in yield stress can be attributed in part to the conformational transitions of the cyclohexylene group, which are motions found to be associated with the secondary relaxation of these copolymers. We believe, on the basis of these findings and results from our previous study,[18] that cooperative motions of the cyclohexylene rings of adjacent repeat units produce lateral excursions of chain segments along the backbone which increase dynamic density fluctuations. These segmental motions can reduce barriers to chain slippage. By this process, the molecular-scale motions of the secondary relaxation directly contribute to increasing macroscopic ductility in the copolymers.

The activation volumes and energies of yielding are determined by applying Eyring's model of yielding. An increase in activation volume is calculated, while changes in the activation energy for yielding are not significant. Therefore, for similar activation energies, copolymers of greater cyclohexylene concentration are are able to activate a larger volume during the yield process. We offer the hypothesis that the dynamic fluctuations induced by the cyclohexylene motion makes yielding a more efficient process for these copolyesters.

In addition, the craze stress of the copolyesters increases with increasing cyclohexylene content. We associate the increase with factors affecting nanovoid formation during craze initiation based on a homogeneous nucleation theory. In this theory, the stability of a void is determined by the change in Gibb's free energy due to a surface energy component and a bulk strain energy component. In the case of high cyclohexylene content, we believe the formation of stable nanovoids is impeded by local chain fluctuation which keeps the voids at a subcritical size. That is, the creation of a nanovoid stable enough to induce a macroscopic craze is delayed by molecular fluctuations which collapse the void. Such fluctuations are clearly indicated by the PALS results.

With an understanding of how the cyclohexylene motion can affect yielding and crazing, we describe the ductile/brittle transition as a competition between yielding and crazing and attribute changes in the transition temperature ultimately to molecular motions of the cyclohexylene groups. We have also presented an alternative means to view the ductile−brittle transition temperature, namely by constructing failure envelopes outlined by the shear and dilative failure stresses. This is useful for understanding the effectiveness of rubber toughening. This study shows a direct correlation between motions of the secondary relaxation and mechanical behavior for PET/PCT copolymers.

Acknowledgment. This work was supported by grants from the Eastman Chemical Co. and the National Science Foundation, Grant DMR-9422049. The Eastman Chemical Co. supplied the polyesters used in this study.

References and Notes

(1) Boyer, R. F. *Polym. Eng. Sci.* **1968**, *8*, 161.
(2) Heijboer, J. *J. Polym. Sci., Part C* **1968**, *16*, 3755.
(3) Sacher, E. *J. Appl. Polym. Sci.* **1975**, *19*, 1421.
(4) Wada, Y.; Kasahara, T. *J. Appl. Polym. Sci.* **1967**, *11*, 1661.
(5) Vincent, P. I. *Polymer* **1974**, *15*, 111.
(6) Glover, A. P.; Johnson, F. A.; Radon, J. C. *Polym. Eng. Sci.* **1974**, *14*, 420.
(7) Kastelic, J. R.; Baer, E. *J. Macromol. Sci., Phys.* **1973**, *B7*, 679.
(8) Xiao, C.; Jho, J. Y.; Yee, A. F. *Macromolecules* **1994**, *27*, 2761.
(9) Xiao, C.; Yee, A. F. *Macromolecules* **1992**, *25*, 6800.
(10) Vincent, P. I. *Polymer* **1960**, *1*, 425.
(11) Ree, T.; Eyring, H. *J. Appl. Phys.* **1955**, *26*, 793.
(12) Bauwens-Crowet, C.; Bauwens, J. C.; Homes, G. *J. Polym. Sci., Polym. Phys. Ed.* **1969**, *7*, 735.
(13) Roetling, J. A. *Polymer* **1965**, *6*, 311.
(14) Bauwens, J. C. *J. Mater. Sci.* **1972**, *7*, 577.
(15) Foot, J. S.; Truss, R. W.; Ward, I. M.; Duckett, R. A. *J. Mater. Sci.* **1987**, *22*, 1437.
(16) Kramer, E. J. *Adv. Polym. Sci.* **1983**, *52/53*, 1.
(17) Kramer, E. J.; Berger, L. L. *Adv. Polym. Sci.* **1990**, *91/92*, 1.
(18) Chen, L. P.; Yee, A. F.; Goetz, J. M.; Schaefer, J. *Macromolecules* **1998**, *31*, 5371.
(19) Jean, Y. C. *Microchem. J.* **1990**, *42*, 72.
(20) Hristov, H.; Bolan, B.; Yee, A. F.; Xie, L.; Gidley, D. *Macromolecules* **1996**, *29*, 8507.
(21) Hill, R. *The Mathematical Theory of Plasticity*; Oxford University Press: New York, 1950.
(22) Allison, S. W.; Ward, I. M. *Br. J. Appl. Phys.* **1967**, *18*, 1151.
(23) Lazurkin, J. S. *J. Polym. Sci.* **1958**, *30*, 595.
(24) Robertson, R. E. *J. Appl. Polym. Sci.* **1963**, *7*, 443.
(25) Haward, R. N.; Thackray, G. *Proc. R. Soc. London A* **1968**, *302*, 453.
(26) Brady, T. E.; Yeh, G. S. Y. *J. Appl. Phys.* **1971**, *42*, 4622.
(27) Brady, T. E.; Yeh, G. S. Y. *J. Macromol. Sci., Phys.* **1974**, *B9*, 659.
(28) Heijboer, J. *Kolloid-Z.* **1960**, *171*, 7.
(29) Heijboer, J. In *Molecular Basis of Transitions and Relaxations*; Meier, D. J., Ed.; Gordon and Breach: New York, 1978; pp 297−310.
(30) Ishikawa, M.; Ogawa, H.; Narisawa, I. *J. Macromol. Sci., Phys.* **1981**, *B19*, 421.
(31) Garde, A. M.; Weiss, V. *Met. Trans.* **1972**, *3*, 2811.
(32) Mills, N. J. *J. Mater. Sci.* **1976**, *11*, 363.
(33) Ishikawa, M.; Narisawa, I.; Ogawa, H. *J. Polym. Sci., Polym. Phys. Ed.* **1977**, *15*, 1791.
(34) Narisawa, I.; Ishikawa, M.; Ogawa, H. *J. Mater. Sci.* **1980**, *15*, 2059.
(35) Narisawa, I.; Yee, A. F. In *Materials Science and Technology, A Comprehensive Treatment*; Cahn, R. W., Haasen, P., Kramer, E. J., Eds.; VCH Verlag: Weinheim, 1993; Vol. 12, Chapter 15, pp 699−765.
(36) Fellers, J. F.; Kee, B. F. *J. Appl. Polym. Sci.* **1974**, *18*, 2355.
(37) Sternstein, S. S.; Onchin, L.; Silverman, A. *Appl. Polym. Symp.* **1963**, *7*, 175.
(38) Gent, A. N. *J. Mater. Sci.* **1970**, *5*, 925.
(39) Argon, A. S.; Hannoosh, J. G. *Philos. Mag.* **1977**, *36*, 1195.
(40) Kausch, H. H. *Kunststoffe* **1976**, *66*, 538.
(41) Rasmussen, G. Eastman Chemical Co., private communication.
(42) Hristov, H. A.; Yee, A. F.; Gidley, D. W. *Polymer* **1994**, *35*, 3604.
(43) Hristov, H. A.; Yee, A. F.; Xie, L.; Gidley, D. W. *Polymer* **1994**, *35*, 4287.
(44) Huang, J.; Shi, Y.; Yee, A. F. *ACS PMSE Proc.* **1994**, *70*, 258.

MA981363A